Ultra fast oscillations in the human brain and their functional significance

Milan Brázdil[1,2,#*], Gregory A. Worrell[3,4,#], Vojtěch Trávníček[5,6], Martin Pail[1,6], Robert Roman[2], Filip Plešinger[6], Petr Klimeš[6], Jan Cimbálník[5], William Stacey[7,8,9], Pavel Jurák[6]

[1]Brno Epilepsy Center, Department of Neurology, St Anne's University Hospital and Faculty of Medicine, Masaryk University, Brno, Czech Republic.

[2]Central European Institute of Technology Masaryk University, Brno, Czech Republic.

[3]Department of Neurology, Mayo Clinic, Rochester, MN, USA

[4]Department of Physiology and Biomedical Engineering, Mayo Clinic, USA.

[5]International Clinical Research Center, St. Anne's University Hospital, Brno, Czech Republic.

[6]The Czech Academy of Sciences, Institute of Scientific Instruments, Brno, Czech Republic.

[7]Department of Neurology, University of Michigan, USA.

[8]Department of Biomedical Engineering, University of Michigan, USA.

[9]Biointerfaces Institute, University of Michigan, USA.

# These authors contributed equally: Gregory A. Worrell, Milan Brázdil

* Corresponding author

Human brain cellular assemblies generate emergent oscillations up to very high frequencies that can exceed the known firing rates of individual neurons. Using advanced intracranial microEEG recordings in a cohort of patients with epilepsy, we identified short-lasting local field oscillations with frequencies between 2 and 8 kHz. These ultra fast oscillations were consistently and locally detected in epileptic hippocampi but were extremely rare in normal brain tissue. The observed ultra high frequency oscillations may reflect local circuit hyperexcitability and we use a simple model to demonstrate the feasibility that these local fields are emergent oscillations representing the crest of collective high frequency neuronal unit activity.

Using direct electrical signal recordings from the human brain via intracranial electrodes, a wide range of frequencies spanning from ultra slow (<0.5 Hz) to very fast oscillations (500-2,000 Hz) have been repeatedly detected (Brazdil et al, 2017; Worrell et al, 2012). All these electrophysiological phenomena can be observed in both healthy and functionally impaired brain structures using standard clinical macroelectrodes (1 - 10 mm2) to record local field potentials that reflected the summated synaptic activity, commonly called intracranial EEG (Buzsáki et al, 2012). In parallel, some studies suggest that the human brain can generate even higher frequencies (above 2 kHz) (Sakura et al., 2009;

Usui et al., 2010; Cao et al., 2014). If this is true, then EEG micro recordings should be a more potent tool to probe for these ultra fast frequency activities, as shown previously (Worrell et al., 2008, Brazdil et al. 2017). The aim of this study was to analyze resting-state intracranial EEG data from intrahippocampal hybrid (macro/micro) depth electrodes in a cohort of patients with epilepsy using high sampling frequencies (25 or 32 kHz). Here we focused on EEG activities in between 2 and 8 kHz. Hypothetical ultra fast electrical events within the human brain might bear distinct functional significance when compared to lower frequencies and possibly could substantially contribute to our better insight into the pathophysiology of epileptic disorder on the microscopic level.

Using a spectrogram based detector, we analyzed EEG data from 161 microcontacts (109 “shafts” and 52 “bundles”=microwires) and 90 macrocontacts of 12 hybrid depth electrodes in total, recorded in eight subjects who were investigated in two independent epilepsy monitoring units. As expected, in both macro- and microcontacts of the depth EEG electrodes implanted into the mesiotemporal structures, and mainly into the epileptic hippocampus, we repeatedly detected high-frequency oscillations (HFOs) in the frequency range of ripples (80-250 Hz) and fast ripples (250-500 Hz). We also detected the recently described very high-frequency oscillations (VHFOs) in a range of very fast ripples (500-1000 Hz) and ultra fast ripples (1-2 kHz). In addition, short-lasting oscillations in frequencies between 2 and 8 kHz were occasionally detected in the microrecordings from all of the investigated subjects. Two distinct types of these ultra fast oscillations (UFOs) could be differentiated and both types were observed in recordings across two independent EEG labs (Fig. 1). Ultra fast oscillations type I had a pattern of typical spindle-like ripples, they were not accompanied by synchronous lower frequency activities, and their mean amplitude was 61.9 ± 26.1 μV. Ultra fast oscillations type II started with an initial “high amplitude” sharp deflection followed by an oscillation rapidly decreasing in its voltage. Also, these UFOs II were not mostly occurring in a parallel with lower frequency activities and mean amplitude was 190.0 ± 71.7 μV. They were less frequent when compared to UFOs I (835 versus 2884,$p<0.001$), and were present in the microrecordings from all but one subject in whom type I “microoscillations” were detected only. Notably, ultra fast oscillations of different frequencies and types co-occur in the individual EEG recordings, in the same or another channel, and they were present asynchronously each to the other (Fig. 1D). The UFO occurrence importantly fluctuated in time. In the time domain, 7.3±6.8 % of ultra fast oscillations overlapped with spikes, and more frequently they overlapped with ripples (17.7±19.1%), fast ripples (15.2±15.2%), and very fast ripples (12.9±10.7%).

Importantly, standard depth macroelectrodes were limited to detection of high frequency oscillations above 2 kHz, except in a single epileptic intrahippocampal macrocontact of one subject out of three with available high-sampling macroEEG data. In this single “comparative” recording, the rate of UFOs in the macrocontact was approx. 50x smaller compared to maximum rate in adjacent microrecordings (0.08/min versus 3.8/min).

In our study, ultra fast oscillations were consistently and locally detected in microrecordings from epileptic hippocampi (in all five available intrahippocampal recordings), and once from a neocortex microelectrode adjacent to the epileptic hippocampus. A maximum of microscillations was observed here in the frequency range 2-5 kHz, but in two subjects they reached up to 7, and 8 kHz, respectively. The UFO rates varied inter-individually, across time and across recording microcontacts, with a maximum rate 3-7.9/min for most active channels within three definitely epileptic hippocampi (successfully operated). The ultra fast oscillations were present both widely across several recording

microcontacts (generally in lower frequency ranges, 2-3 kHz) as well as more locally, and repeatedly even in a single contact (in higher frequency ranges). Importantly, Type I and Type II of ultra fast oscillations obviously did not represent the identical phenomenon, even if both of them predominantly affected similar channels (Fig. 2). Finally, parallel recordings from adjacent macrocontacts consistently revealed traditional HFOs and VHFOs. In contrast to recordings from epileptic hippocampi, no convincing or extremely rare ultra fast oscillations were detected in microrecordings from undisputed non-epileptic hippocampi (N=2).

Despite a prevailing assumption that ultra fast EEG activity has its limitation at around 1,000 Hz and faster frequencies might be nothing but "neuronal chatter" (Niedermeyer, 2005), several papers published in the last decades are telling us the opposite. A novel ultra fast electrophysiological component of somatosensory-evoked potentials (1,235 - 2,632 Hz) was directly recorded from the human brain by Sakura et al. (2009) and even with higher frequencies by Cao et al. (2014). Two other independent research groups provided convincing proof of non-event very high frequency oscillations up to 2,000 Hz in the human epileptic brains (Usui et al., 2010, 2015; Brazdil et al., 2017). By analogy, high frequency activities at 2,000 Hz were identified in *in vivo* intrahippocampal electrophysiological recordings from a rat using a novel pseudo-wavelet approach, and these activities increased in prominence with epileptogenesis (Hsu et al., 2010). And finally, even a specialized electric organ of weakly electric fish *Apteronotus leptorhynchus* comprising neuron-like cells is able to produce physiological and intentional discharges up to 2.2 kHz (Albert and Crampton, 2005). Our observation of ultra fast oscillations in the frequencies between 2 and 8 kHz, recorded using microelectrodes mostly from the human epileptic hippocampi and their surroundings, can be seen as the next breakthrough step moving the limits of electroencephalography and our understanding of electrical events in the human brain. Microelectrodes have much higher impedance than macroelectrodes and are highly prone to artifacts (Stacey et al., 2013). Thus our analyses were done with great care and it seems to be highly unlikely we faced some kind of "false" HFOs. The origin of SEEG data in two independent labs across the world and two distinct EEG recording systems, together with intra individually selected observations across all investigated subjects, characteristics of the events, and obvious predilection of ultra fast oscillations to epileptic tissue, make the artificial provenance of UFOs hardly possible.

Scepticism on the authentic origin of UFOs might be nevertheless augmented with our knowledge of an absolute inactive phase of neurons at about 2 msec. A single synchronized neuronal group can generate discharges with the upper limit at about 300 Hz. On the other hand, the network mechanisms underpinning fast ripple and faster oscillations could be explained by phase delay of different subpopulations of synchronized neurons, i.e. out-of-phase firing (Jiruska et al., 2017). Such desynchronized subpopulations can fire with frequencies up to 500 Hz or even higher. The computational model presented recently by Fink et al. (2015) showed a similar effect on cellular level with a simulated cluster of asynchronous, uncoupled network of pyramidal cells. When the inhibitory mechanisms in the neural tissue are impaired and the pyramidal cells become very active due to intense synaptic input, the multiunit out-of-phase firing can occur and produce very high frequencies, very likely far more than 1,000 Hz. When the pyramidal cells are desynchronized the aggregate electrophysiological signal can result in ultra fast oscillations of any frequency which detection is then only limited with an advancement of recording devices.

To conclude, in this study, we describe for the first time ultra fast electric field oscillations above 2 kHz in the human brain. These electrophysiological events can be reliably detected using advanced depth microEEG recordings and they likely mirror neuronal hyperexcitability and reflect the hypersynchronous firing of neurons and a collective oscillation created by summation of the crests of single unit neuronal firing activity As such, their future studies may provide a deeper insight into the pathomechanisms of epileptogenic brain.

References

Albert J. S., Crampton W. G. R. (2005). Diversity and phylogeny of neotropical electric fishes (Gymnotiformes). In *Electroreception* (ed. Bullock T. H., Hopkins C. D., Popper A. N., Fay R. R.), pp. 360-409. New York, NY: Springer.

Brazdil M, Pail M, Halamek J, et al. Very high-frequency oscillations: Novel biomarkers of the epileptogenic zone. Ann Neurol. 2017;82(2):299-310.

Buzsáki, G, Anastassiou CA, Koch C. The Origin of Extracellular Fields and Currents--EEG, ECoG, LFP and Spikes. Nature Reviews. Neuroscience 2012;13(6):407–20.

Cao D, Terada K, Baba K, et al. Characteristics of very high frequency oscillations of somatosensory evoked potentials in humans with epilepsy. Neurology Asia. 2014;19(2):137-148.

Fink CG, Gliske S, Catoni N, et al. Network Mechanisms Generating Abnormal and Normal Hippocampal High-Frequency Oscillations: A Computational Analysis. eNeuro May-Jun 2015;2(3):ENEURO.0024-15.2015.

Hsu D, Hsu M, Grabenstatter HL, et al. Time-frequency analysis using damped-oscillator pseudo- wavelets: application to electro- physiological recording. J Neurosci Methods 2010;194:179–192.

Jiruska P, Alvarado-Rojas C, Schevon CA, et al. Update on the mechanisms and roles of high-frequency oscillations in seizures and epileptic disorders. Epilepsia 2017;58(8):1330-1339.

Niedermeyer E. Ultrafast EEG activities and their significance. Clinical EEG and Neuroscience 2005;38(4):257-262.

Sakura Y, Terada K, Usui K, et al. Very high frequency oscillations (over 1000 Hz) of somatosensory-evoked potentials directly recorded from the human brain. J. Clin. Neurophysiol. 2009;26:414-421.

Stacey WC, Kellis S, Gregar B, et al. Potential for unreliable interpretation of EEG recorded with microelectrodes. Epilepsia 2013;54(8):1391-1401.

Usui N, Terada K, Baba K, et al. Very high frequency oscillations (over 1000 Hz) in human epilepsy. Clin Neurophysiol. 2010;121:1825–1831.

Usui N, Terada K, Baba K, et al. Significance of very-high- frequency oscillations (over 1,000Hz) in epilepsy. Ann Neurol. 2015;78:295–302.

Worrell GA, Gardner AB, Stead SM, et al. High-frequency oscillations in human temporal lobe: simultaneous microwire and clinical macroelectrode recordings. Brain 2008;131:928-937.

Worrell, GA, Jerbi K, Kobayashi K, Lina JM, Zelmann R, and Le Van Quyen M. "Recording and Analysis Techniques for High-Frequency Oscillations." Progress in Neurobiology 2012; 98(3):265-278.

Figure Legends

Figure 1: Visualization of raw signals with ultra fast oscillations in different spectrogram settings (median normalization used in all the time frequency maps in the paper) (A)**, examples of types I and II (**time frequency maps and correlating raw EEG data) (B)**, relative rates of spikes, ripples, fast ripples, very fast ripples, ultra fast ripples and UFOs** across all multi subject microrecordings (C)**, and example of mutual temporal relationships of distinct oscillations in two selected adjacent and simultaneous microrecording channels** (D)

Figure 2: Distribution of UFR (1-2 kHz) and UFOs (2-8 kHz) across microcontact recordings in four investigated patients (A-D) . For each subject one electrode data are shown only. **A,C - epileptic hippocampus, B - non-epileptic hippocampus, and D - epileptic entorhinal cortex.** Event detections for each microcontact in time are given in color strips reflecting the event type (I, II or both). Each strip is representing 1 sec time interval with at least one (or more) microoscillation.

Figure1:

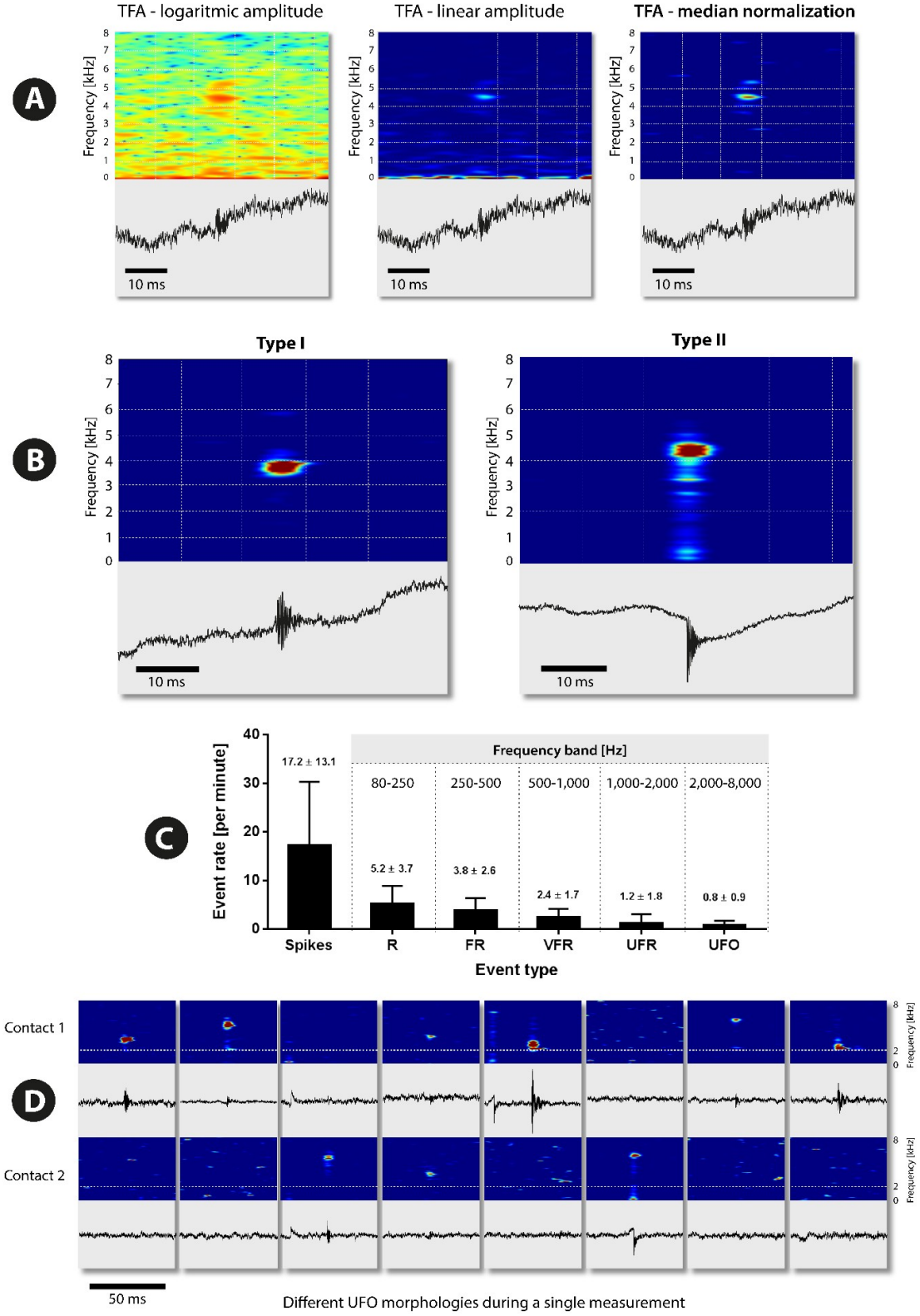

Different UFO morphologies during a single measurement

Figure 2:

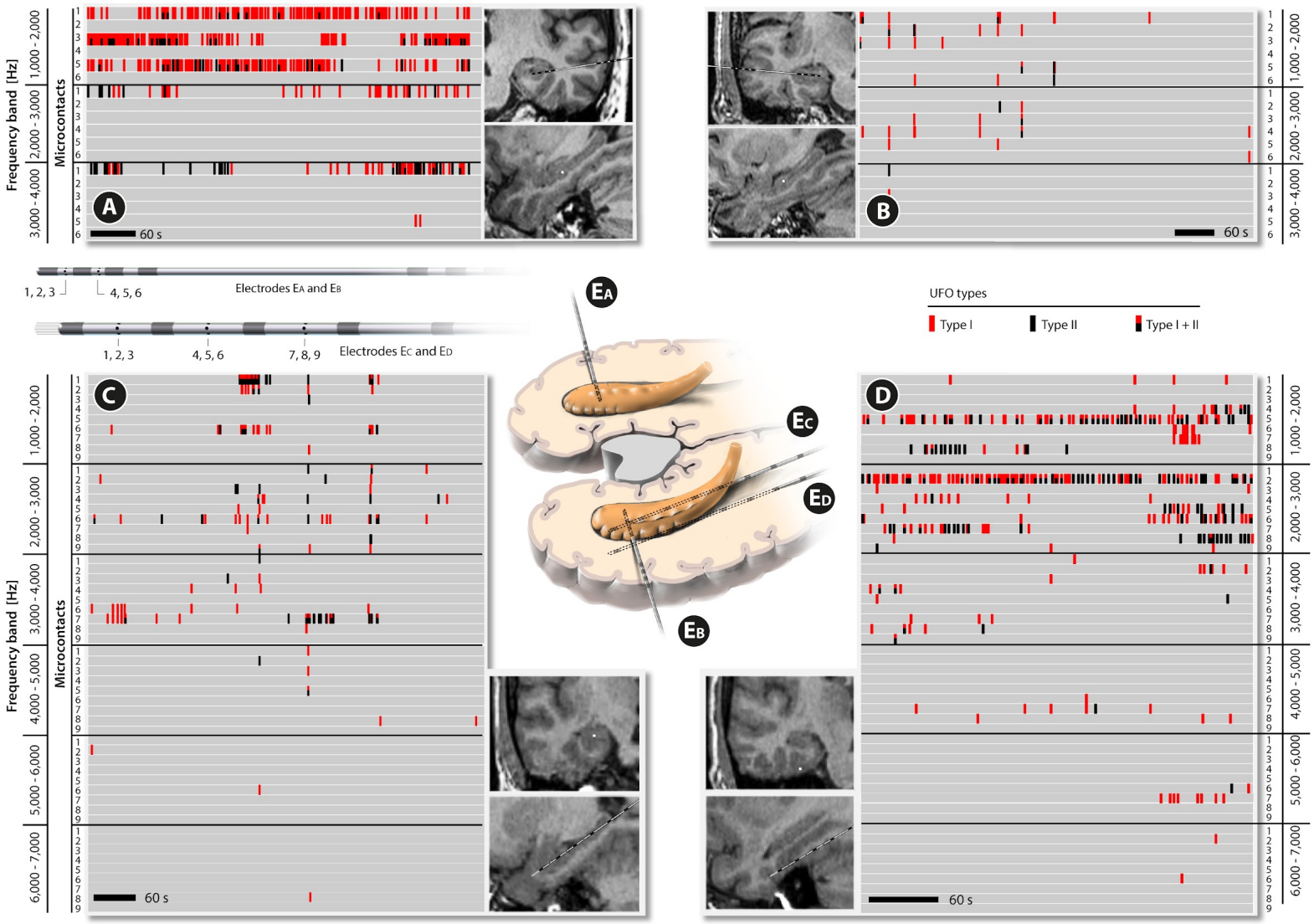
A
B
C
D
Frequency band [Hz]
1,000 - 2,000
2,000 - 3,000
3,000 - 4,000
4,000 - 5,000
5,000 - 6,000
6,000 - 7,000
Microcontacts
60 s
1, 2, 3
4, 5, 6
7, 8, 9
Electrodes EA and EB
Electrodes EC and ED
EA
EB
EC
ED
UFO types
Type I
Type II
Type I + II

Table 1: Relative rates of microoscillations (p/m) for ultra fast ripples (1-2 kHz) and ultra fast oscillations (2-8 kHz). Three proven epileptic and two non-epileptic hippocampi, each row for one microcontact recording. High rates (>3) are highlighted; high UFR rates have a blue background, high UFO rates have an orange background.

			Frequency [Hz]						
		Contact	1-2kHz	2-3kHz	3-4kHz	4-5kHz	5-6kHz	6-7kHz	7-8kHz
Epileptic hippocampi	Patient 5	1	3.6	0.7	7.9	0	0	0	0
		2	0.1	0.2	0	0	0	0	0
		3	16.5	0	0.1	0	0	0	0
		4	0.1	0	0.7	0	0	0	0
		5	6.5	0.1	0.4	0	0	0	0
		6	0	0	0	0	0	0	0
	Patient 4	1	0.6	1.2	0.3	0	0	0	0
		2	1.3	2	0.3	0.4	0	0	0
		3	0.3	0.4	0.4	0.3	0.1	0	0
		4	2.8	2	0.4	0.1	0	0	0
		5	1.9	3	2.5	0.2	0.1	0.1	0
		6	3.8	2.4	0.3	0.2	0.1	0	0
	Patient 3	1	0.2	0	0	0	0	0	0
		2	0	0.2	0	0	0	0	0
		3	2.4	0	0	0	0	0	0
		4	0.2	0	0	0	0	0	0
		5	0.6	0	0.2	0	0	0	0
		6	0	0	0	1.6	0.2	0	0
		7	0.2	0.2	0	0	0	0	0
		8	0	0.2	0	0	0	0	0
		9	1	0	0	0	0	0	0
		10	0.4	0	0	0	0	0	0
		11	0	0	0.2	0	0	0	0
		12	0.2	0	0	0	0	0	0
		13	0	0	0	0	0	0	0
		14	0	0	0	0	0	0	0
		15	0.4	0	0.2	0	0	0	0
		16	1.4	3	3.4	0.2	0.6	0	0
Non-epileptic hippocampi	Patient 2	1	1.1	0	0.3	0.2	0	0	0
		2	1	0.2	0	0	0	0	0
		3	1.8	0.6	0.1	0.1	0	0	0.1
		4	0	1.8	0	0	0	0	0
		5	0.5	0.2	0	0	0	0	0
		6	0.3	0.3	0	0	0.1	0	0
	Patient 1	1	0	0.4	0	0	0	0.2	0
		3	0.2	0	0	0	0	0	0
		4	0	0	0.2	0	1	1.2	0.4
		5	0	0.4	0	0	0	0	0
		6	0	0	0.2	0	0	0	0
		7	0.2	0	0	0	0	0	0
		8	0.2	0	0.2	0	0	0	0
		9	1	0	0	0.2	0	0	0

Online Methods

Patients

Eight consecutive patients (4 males; 4 females) with drug resistant focal temporal lobe epilepsy (DRE: Commission on Classification and Terminology of ILAE, 1989) who underwent presurgical evaluation using intracranial stereo EEG recordings (stereo-electroencephalography, SEEG) with at least one hybrid depth electrode were consented and included in the study. All of them suffered from focal impaired awareness seizures and one of them additionally (plus) from focal to bilateral tonic-clonic seizures. Five patients were recorded in Mayo Clinic, Rochester, U.S.A. and three patients were investigated in Brno Epilepsy Center, Czech Rep., E.U. Subjects ranged in age from 22 to 53 years (mean age 37.5 years, SD = 11.4). The main demographic and clinical characteristics of the involved subjects are shown in the Table.

Table Patients' demographic and clinical characteristics

Subject	Gender	Age at Seizure Onset	Age at SEEG	Seizure Frequency/Monthly	MRI (signs of)	Implanted hybrid electrodes	Type and side of epilepsy	SOZ	Surgery/ histopathology	Outcome (Engel) (years)
1	F	16-20	46-50	2	normal	RT	T / R	right hippocampus (B2-3)	right AMTR/gliosis	IA (5)
2	M	21-25	26-30	30 plus	posttraumatic changes left lateral T	LT	T/ L	left lateral T neocortex (S´4-7)	left lateral T lesionectomy/ posttraumatic changes	ID (4)
3	M	31-35	51-55	4	left HS	LT	T / L	left hippocampus (B´1-3)	left AMTR/HS	ID (3)
4	F	0-5	26-30	1	bilat HS	RT, LT	T / bilat	bilateral; left and right hippocampus (LTD1-3, RTD1-3)	NA	
5	M	16-20	36-40	8	normal	LT	T / L	left hippocampus (LAD1-3)	left AMTR/gliosis	IA (7)
6	M	36-40	46-50	4	normal	RT, LT	T / bilat	bilateral; left and right hippocampus (LTD1-4, RTD1-4)	NA	
7	F	0-5	21-25	4	left HS	LT, RT	T / L	left hippocampus (LTD1-2)	left AMTR/HS	IC (8)
8	F	16-20	31-35	6	normal	RT	T / R + E / L	right hippocampus (RDT1-4) + left extratemporal (:::)	NA	

All patients underwent a comprehensive presurgical evaluation, including a detailed history and neurological examination, brain magnetic resonance imaging (MRI), neuropsychological testing, and scalp and invasive video-EEG monitoring. The duration of clinical monitoring and the location and number of implanted electrodes were determined in accordance with clinical considerations. After invasive videoEEG monitoring five patients underwent surgical intervention details of which are shown in Table 1. The follow-up interval after epilepsy surgery was at least 3 years. The study was approved by Mayo Clinic Internal Review Board, the St. Anne's University Hospital Research Ethics Committee, and the Ethics Committee of Masaryk University. All patients signed an informed consent form.

SEEG recordings

In Mayo Clinic, custom hybrid depth electrode designs (AD-Tech Medical Instrument Corporation, Racine, WI) were used. These electrodes are based on standard four and eight contact clinical depth electrodes. The depth electrodes consist of a 1.3 mm diameter polyurethane shaft with Platinum/Iridium (Pt/Ir) clinical macroelectrode contacts; each clinical contact is 2.3 mm long with either a 5 or 10 mm center-to-center spacing (surface area 9.4 mm^2). In addition to the standard clinical contacts, the 8 contact depth has 8-24 microcontacts (between 1-4 macrocontacts), and the 4 contact depth has 16 microcontacts, positioned radially along the shaft of the depth electrode. Each electrode has a bundle of 9 Pt/Ir microwires that protrude 1–3 mm from the shaft tip. The microwires are made of insulated Pt/Ir wire, 40 um in diameter.

The patients received one hybrid SEEG electrode in the temporal lobe bilaterally and in one patient subdural strips and other intracerebral electrodes were implanted for monitoring of the parietal and occipital lobe. The electrode position within the brain was verified using CT with electrodes in situ.

A clinical acquisition system (Neuralynx Inc., Bozeman MT) was used to acquire intracranial EEG at Mayo Clinic. The signal was acquired at 32 kHz sampling frequency. Macro EEG was subsequently filtered by Barlett-Hanning 1 kHz low pass filter and downsampled to 5 kHz sampling frequency. The stainless steal suture placed in the vertex region of the scalp midline between the international 10–20 Cz and Fz electrode positions was used as a common reference.

In Brno Epilepsy Center, aside standard depth multi-contact platinum electrodes with a diameter of 0.8mm, a macrocontact length of 2mm, and an intercontact distance of 1.5mm (Microdeep, DIXI Medical, Besançon, France or Depth Electrodes Range, ALCIS, Besançon, France), one custom hybrid depth electrode (2069-ECP-8C6-35T06-2G-26, ALCIS, Besançon, France) was used in each subject. This electrode has eight macrocontacts (each with surface area of 5mm^2) and six microcontacts positioned radially along the shaft (surface area of 1075 μm^2) interspersed between 1. and 3. macrocontacts (Fig. 2). Each patient received 3 to 14 depth electrodes usually orthogonally in the temporal and facultatively in frontal lobes. Their position within the brain was verified using MRI and CT with electrodes in situ.

A 192-channel research EEG acquisition system (M&I; BrainScope, Prague, Czech Republic) was used for recording of 30 minutes of awake resting interictal SEEG recordings with a sampling rate of 25 kHz and dynamic range of +-25mV. The EEG acquisition unit was battery powered to eliminate line noise and microelectrodes were connected to specialized high impedance amplifiers (>1 GΩ). We used standard epilepsy monitoring unit protocols, but emphasis was given to eliminating power sources of electromagnetic radiation and 50 Hz power grid influence. No special shielded environment was used. Ground electrode served as a reference for microcontacts, mean from all macrocontacts was used as a reference for macrocontacts.

All data processing was performed using open platform software SignalPlant and Python software. Signal-Plant was used for interactive graphical analysis of large, multi- channel data. Custom Python scripts were used for batch processing of data and statistics.

Detection methods

Oscillations above 1 kHz

Detection was performed in a 30 sec sliding window. First, a spectrogram of the input signal was computed with the FFT window of 0.015s with 97% overlap and detrending of the windowed signal. Every row of the spectrogram was divided by its median (normalized) in 1 sec sliding window (Fig 3B). Only frequencies 1-8 kHz were taken into account. Higher frequencies might include artefacts from the recording system and events from lower frequencies are out of the scope of this analysis. One dimensional detection signal was created by summing all rows of the filtered and frequency-bounded (1,000 – 8,000 Hz) spectrogram. 99 percentile multiplied by factor of 5 was used for peak detection on the one dimensional signal (Fig 3C). Peak areas bounded by its inflex points were marked as high frequency activity. For each putative oscillation detection two things were saved for further analysis:

1) Original raw signal of the putative detection

2) Spectral profile created by summing all columns of normalized spectrogram within time-bounded detection area (Fig 3E)

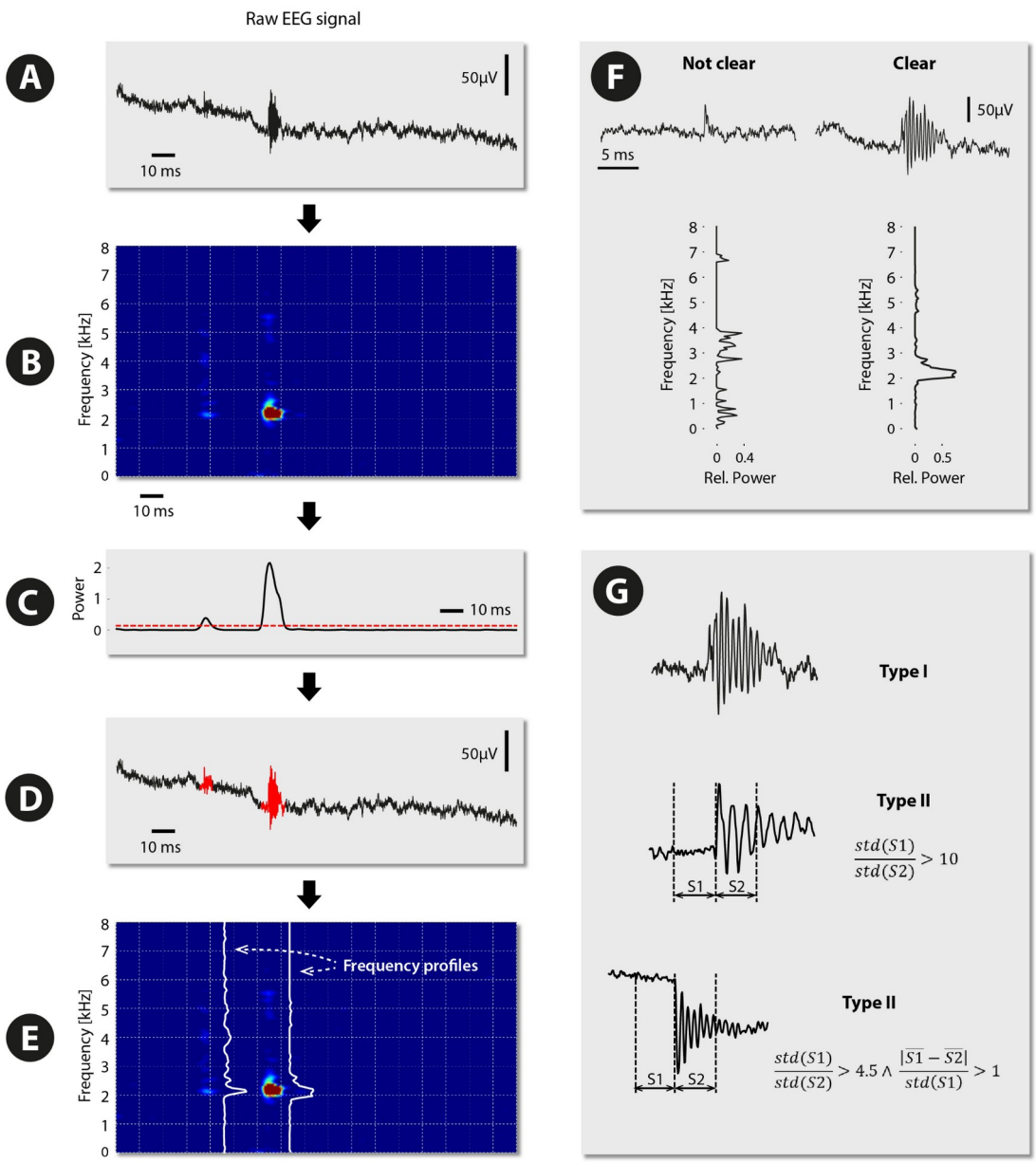

Figure 3: The figure introduces the UFO detection method. Primary detection of every high-frequency activity is depicted in the left panel. Part A) shows the raw signal. Its' normalized spectrogram is in the B) part. Summing all rows of the spectrogram creates a 1-dimensional detection signal, which is thresholded (part C). D) part of the picture shows primary detections; its spectral profiles are shown in the E) part. The right panel shows filtering of primary oscillations. First, oscillations are assessed regarding their spectral profile as clear or not clear, which are removed from further analysis F). Other oscillations are sorted into two groups (part G).

Every spectral profile of a detected high frequency event was subsequently classified either as biological or noisy. Event was marked as biological if the ratio of maximum to mean of the spectral profile was greater than 10. Other profiles were marked as noise because there was no dominant

frequency and therefore could be considered as wide spread noise. Maximum to mean ratio served as the tuning parameter of the detector and was chosen heuristically. Lowering this number led to more detections, however their main frequency was less dominant. By setting this parameter to the value of 10, we chose 34.8±22.1% of primary detections, depending on the record (Fig 3F).

We observed that there were two major shapes of oscillations, Type I was fluently increasing and decreasing its amplitude and oscillates in one frequency band, which was represented by one circular or ellipsoidal area in spectrogram, while Type II oscillation started with sudden increase followed by slow decrease of amplitude often accompanied by shift of mean amplitude (see Fig. 3G bottom). This behavior led into one vertical strip in the spectrogram followed by high activity in one frequency area. To distinguish between these two shapes, the raw signal of every detection bounded by detection start and end was analysed. The point where the absolute value of the derivative reached half of its maxima was marked as a True detection start. ¼ of detection length to the left from True detection start was marked as section 1 and ¼ of detection length to the right was marked as section 2. If the True start was not placed between ¼ and ¾ length of the detection it was automatically categorized as Type I. The nature of the detector (length of FFT window, using inflex points for detection start) ensures that Type II oscillations were always detected prior to their typical amplitude rise. Type II oscillation was defined by either of the following:

1. $$\frac{std(section2)}{std(section1)} > 10$$
2. $$\frac{std(section2)}{std(section1)} > 4.5 \wedge \frac{\left|(mean(section1) - mean(section2))\right|}{std(section1)} > 1$$

Equation 1. represents sudden change in standard deviation of amplitude within oscillation. So does equation 2., but one condition added, which represents a shift of means between two sections. Clear oscillations that did not fulfill any of these conditions were marked as Type I. Constants 10 and 4.5 can be considered as tuning parameters and were chosen heuristically. Using these constants we categorized apr. 35% of oscillations as Type II and 65% oscillations as Type I.

In some cases, the UFOs were detected simultaneously in more than three microcontacts at the same time. We declared these detections artefacts and omitted them from statistics, because there is a risk that these oscillations are caused by electrode movement. 42% of all detections were declared artifacts.

To statistically compare the absolute count of Type I and Type II oscillation, we used non-parametric paired Wilcoxon signed-rank test, where oscillation count on each patient channel served as one sample.

Ripples, fast ripples and very fast ripples

Oscillations in ripple (80-250 Hz), fast ripple (250-500 Hz) and very fast ripple (500-1000 Hz) bands were detected using Line-length detector (Gardner et al. 2007). For every oscillation type, signal was first processed by 3rd order band-pass filter in respective band, detection was performed by Line-length detector with following parameters: the statistical window of 10 sec, 6 standard deviations was set as the detection threshold, window size was calculated as fs/50 samples, where fs stands for sampling frequency, window overlap was set to 25% of the sliding window length

Spikes

Barkmeier detector (Barkmeier et al. 2012) was used for spike detection with following parameters: scale factor 70, threshold coefficient of 4 standard deviations, left and right slope ratios of 700, left and right spike duration of 0.1 second.